

Research Article

Specific Surface Area Enhancement of Waste Tire-Based Activated Carbon by Demineralization Technique and Adsorption of Methylene Blue

Estifanos Kassahun ¹, Sintayehu Mekuria ¹, and Surafel Mustefa Beyan ²

¹Department of Chemical Engineering, Food and Beverage Industry Research and Development Center, College of Biological and Chemical Engineering, Addis Ababa Science and Technology University, Addis Ababa, Ethiopia
²School of Chemical Engineering, Jimma Institute of Technology, Jimma University, Jimma, P.O. Box 387, Ethiopia

Correspondence should be addressed to Sintayehu Mekuria; sintayehu.mekuria@aastu.edu.et and Surafel Mustefa Beyan; surafel.beyan@ju.edu.et

Received 1 February 2022; Revised 30 May 2022; Accepted 29 June 2022; Published 1 August 2022

Academic Editor: Senthil Kumar Ponnusamy

Copyright © 2022 Estifanos Kassahun et al. This is an open access article distributed under the Creative Commons Attribution License, which permits unrestricted use, distribution, and reproduction in any medium, provided the original work is properly cited.

This study was focused on the synthesis of activated carbon from a waste tire and the enhancement of its specific area by a demineralization technique that can be used for the removal of methylene blue dye (MB). Maximum MB removal (89.41%) was attained at an impregnation ratio value of 0. A maximum yield (42.65%) was found at 48 h. Waste tire-based activated carbon (WTAC)'s ability to remove MB was increased by large values up to an impregnation time of 24 h. WTAC has a maximum MB removal of 90.13% at 4 M of KOH. The sample had a surface area of 53 m²/g. This sample was demineralized by using NaOH and H₂SO₄ in a 1 : 1 ratio, and the surface area was enhanced to 257 m²/g. In the demineralization process, a massive decrement of metals from the waste was seen; for each metal, namely, Zn²⁺, Al³⁺, Ca²⁺, and Mg²⁺, 43.79%, 32.45%, 27.95%, and 6.843% reductions were achieved, respectively. After this process, the maximum removal of MB was found at 1.2 g adsorbent dosage, 120 min, pH 8, the temperature of 20°C, and an initial dye concentration of 10 mg/L. The adsorption mechanism revealed that the process of adsorption happens at a specific site of homogeneous adsorption on the surface of the adsorbent. The kinetics study showed that the adsorption process of the dye is mainly affected by the chemical reaction.

1. Introduction

Activated carbon (AC) is one of the adsorbent substances, which are prepared from carbon-containing sources. Because of its high degree of microporosity, activated carbon is frequently employed for a variety of purposes due to the enormous surface area accessible for adsorption or chemical reactions. Because of the high interior surface area and porosity created during carbonation, it has a high adsorption capacity [1, 2]. The presence of activating agents and carbonation conditions influenced the development of pore structures. Activated carbon is used in many industrial applications of separation and purification technologies, catalyst processes, biomedical engineering, energy storage, transporting agent, etc. The extensive availability of active

carbon as an adsorbent, high performance, surface reactivity, and versatility in modifying its chemical and physical characteristics to synthesize adsorbents is the primary reasons for its importance as an adsorbent [3, 4].

In the synthesis of AC, the main important factors taken into consideration are the properties of the precursor. As much as possible, choosing low-cost, easily available, and renewable by-product and waste material is preferable [5]. A car tire waste is one such option. Modern air-filled tires are composed of natural and synthetic rubber, carbon black, metals, and other additives. Tires are technological wonders, with a plethora of various components and compounds to withstand the rigors of heat and cold, high speed, abrasive conditions, and sometimes insufficient air pressure. Tires are made for the use of vehicles; they are not made as a recycling

industry feedstock. Their composition makes it difficult to recycle [6, 7].

Globally, about 1.5 billion waste tires are generated annually. In addition to the annual continuous flow of waste tires, billions of tires are already stocked in piles. In Ethiopia, the amount of waste tires generation is expected to grow with the increase in the vehicle number in the country and the development of infrastructure throughout the country [8]. Thus, these waste tires can be used as a precursor for the development of activated carbon, which in turn can be used for wastewater treatment applications.

Various wastewater remediation-based research studies had been undertaken as an instance-enriched MWCNTs (multiwalled carbon nanotubes) decorated with silica-coated spinel ferrite nanocomposite [9], low-cost biosorbents from fungi [10], and nonmagnetic and magnetic hydrochar [11] to sequester toxic posttransition metallic ions.

Methylene blue (MB) contaminated wastewater is one of the several problems of the residents who live in the vicinity of the textile industries [12]. MB contaminated wastewater affects both terrestrial and aquatic environments including soil, algae, fishes, and other living and nonliving components of the environment. MB contaminated wastewater has both acute and chronic effects depending on the rate of exposure and its level of concentration in the wastewater to human skin. Among such acute and chronic effects, allergic, dermatitis, skin irritation, cancer, and mutation are the major ones [13]. Wastewater discharged from textile industries needs to be treated before it is discharged to the environment.

To remove such harmful substances from wastewater, industrial and municipal sources, several wastewater treatment techniques were developed and used as part of physical approaches. Membrane separation processes [14, 15], ion exchange [16, 17], and adsorption methodologies [2, 18–23] are among the most often employed methods. Each has its own set of benefits and drawbacks [24]. The disadvantage of ion exchange is that the resins are ineffective for various kinds of dyes, with the advantages of having no damage to adsorbent while regeneration. Electrokinetic coagulation yields poor outcomes with acidic dyes and the increased price of the ferrous sulfate and ferric chloride. Membranes are unable to tolerate tough conditions such as high temperatures, reactive surroundings, and dirty feed, hence they are not used as a separation technique by manufacturers [1]. Adsorption, on the other hand, is the preferred wastewater treatment approach because it is simple and easy to use, and it is effective in treating wastewater since it has high efficiency in decolorizing, deodorizing, detoxifying, and rapidly removing hazardous components from wastewater. Microporous materials are used in adsorption-based technologies, which are a potential cost-effective technology that is widely recognized as the most attractive, efficient, and cost-effective due to its ease of low operating and capital investment costs and enhanced energy efficacy [2, 5, 25].

The general objective of the study is to remove methylene blue from synthetic solution by using activated carbon prepared from waste vehicle car tires and to examine the characteristics of the prepared activated carbon and the raw material through different instrumentations. Particularly,

the study aims to achieve the following objectives: (i) To prepare powdered activated carbon from waste vehicle tires by undertaking one variable at time experimentation and then indicate the optimum parameters through central composite design. (ii) To enhance the surface area of prepared activated carbon by the demineralization process. Demineralization on AC helps to dissolve a soluble component from an insoluble solid, where the soluble ash inorganic minerals will be separated from the insoluble, rigid, and carbonaceous AC. In doing so, the specific surface area of the AC can be increased. (iii) To examine the application of prepared activated carbon on synthetically prepared methylene blue dye up to extending different adsorption curves such as adsorption isotherm and kinetics for different samples.

2. Materials and Methods

2.1. Materials and Chemicals. The waste tires were purchased from Addis Ababa, Ethiopia. It was size reduced and brought to the laboratory using a plastic bag. High power electric motor was used to mill the tire to a size of 0.5–1 mm. Sieve was used to having a proportional size distribution. Impregnating and mixing were held using different-sized Petri dishes. Weight measurements were taken by electronic balance. Putting into the copper oven was implied for drying and moisture removal of the sample. Calibrated pH meter and conductivity meter were used to perform acidity, basicity, and conductivity measurements. The filter paper (Whatman, 150 mm Ø) was used for the solid-liquid separation process in both preparation and adsorption of MB. A furnace equipped with a digital display was selected for the carbonization process, which was connected to a nitrogen gas cylinder at one end with the hose. The surface area of the waste tire-based activated carbon (WTAC) was investigated using the Brunauer–Emmett–Teller (BET) (HORIBA Scientific, SA-9600, Japan) surface area analyzer. The morphological structures of WTAC were perceived using a SEM (scanning electron microscope (INSPECT-F50, Germany). UV spectrophotometer (JASCO V-770, Italy) was employed to measure the absorbance of a solution to find out the concentration.

All of the chemical reagents used in these experiments were of analytical quality and acquired from HiMedia. The MB (HiMedia, India) stock solution (2000 mg/L) was prepared by dissolving 2 g of pure MB in 1000 mL of ultrapure water. For pH adjustments, hydrochloric acid (HCl) and sodium hydroxide (NaOH) (HiMedia, India) were utilized. Standard iodine solution was prepared from the dissolution of an appropriate amount of iodide (HiMedia, India) with deionized water and standardized with sodium thiosulfate.

2.2. Preparation of Waste Tire-Based Activated Carbon. Pyrolysis/carbonization of the pretreated tires waste was accomplished in the existence of reagents namely potassium hydroxide (KOH) (HiMedia, India) and ethanol (C₂H₅OH) (HiMedia, India) [26]. The waste tire samples were impregnated with ethanolic potassium hydroxide before

pyrolysis. Potassium hydroxide is a corrosive chemical that had the capability to interrelate with the carbon atoms, catalyzing the dehydrogenation reactions, which leads to carbon with already developed porosity. Ethanol was used due to its less polarity than water and regarded as organic in nature, and can more easily penetrate the tire particles than water [27]. Therefore, carbons obtained from the impregnation method began with 30 g of tires being mixed with a KOH solution containing C₂H₅OH as the solvent in a 250 mL flask. The mixture was put into an oven operating at a constant temperature. The mixing was completed at 95°C and lasted for different times as required. After mixing, the tire-KOH slurry was then pyrolyzed in a furnace equipped with inert N₂ gas. Pyrolysis was carried out at different temperatures.

The carbonization products have been rinsed upon cooling by stirring for 30 minutes in 150 mL of 0.1 N HCl solution, followed by filtering. After that, the acid-washed sample was leached by combining it with 250 mL of distilled water and filtering the mixtures. The water-carbon combination was leached many times until the pH reached 7. After that, the leached products were dried and autoclaved in a 105°C oven.

2.3. Characterization of WT and WTAC

2.3.1. Thermogravimetric (TGA) Analysis. The thermogravimetric analysis, Shimadzu, DTG - 60H, Germany, was conducted under inert N₂ gas with a temperature range of 50 to 900°C and a maintained heating rate (5°C/min).

2.3.2. XRD Analysis. XRD (Olympus BTX™-528) examination was carried out via Cu-Co through a source of radiation (30 kV and 10 W) with an angle of diffraction (2θ) of 10° to 80°. The value of the threshold for splitting was 4 [21, 28–32]. The crystallinity from XRD information was obtained by employing the Scherrer equation (1) with the aid of Origin 2018b pro software.

$$\text{Crystallinity} = \frac{\text{area of crystalline peaks}}{\text{area of all peaks (crystalline + amorphous)}} \times 100. \quad (1)$$

2.3.3. SEM Analysis. The SEM of the samples was analyzed using a scanning electron microscope to record the surface morphology of the WTAC [29, 30, 33, 34]. For the SEM image, the WTAC was cut into small pieces and fixed on the disc. Then the upper layer of the disc was removed and a very small amount of carbon was placed on the black carbon tape, well fixed just by pressing on the silicon wafer. Finally, the results were taken as an image.

2.4. Demineralization of Carbonized WTAC. Initially, 250 ml solvent of the maximum concentration was weighed, recorded, and placed inside a beaker followed by adding 10 g of WTAC. The hot plate was set to a temperature of 125°C, the beaker containing the solution of

WTAC and the solvent was placed on the hot plate and the mixture was allowed to be stirred by a mechanical stirrer. The beaker was kept in the hot bath on the stirrer for the length of the extraction, which was 60 min. Following the completion of the extraction time, the mechanical stirrer was turned off and the WTAC-lixiviant mixture was poured on filter paper (Whatman, 150 mm Ø). By allowing distilled water to pass through it on filter paper (Whatman, 150 mm Ø), WTAC was properly cleaned. After this process, the demineralized WTAC was placed in the oven for 24 hours at 110°C and then sent to the BET analyzer and ash content determination.

2.5. Adsorption of Methylene Blue by WTAC. The adsorption ability of WTAC could be analyzed by conducting a batch adsorption experiment using a standard MB (C₁₆H₁₈N₃SCL, analytical grade) solution. To investigate the effect of four variables, namely adsorbent dosage, pH, initial dye concentration, and contact time, the adsorption experiment was carried out batchwise. The calibration curve developed at 664 nm was used to calculate the MB concentration at equilibrium. The extent of MB uptake by WTAC samples after the equilibrium was reached (q_e ; mg/g) was calculated by the following expression [19]:

$$\text{MB removal} = \left(\frac{C_o - C_e}{C_o} \right) * 100, \quad (2)$$

$$\text{adsorption capacity} = q_e = \left(\frac{C_o - C_e}{W} \right) * V,$$

where Co (mg/L) is the starting concentration of MB and Ce is the equilibrium concentration of MB. The volume of MB solution in the flask is V (L), and the quantity of activated carbon utilized in the experiment is W (g). Finally, the regeneration study was explored to determine the reusability of the prepared activated carbon in adsorbing methylene blue.

2.6. Adsorption Isotherm. Adsorption isotherms are extremely useful for determining the adsorption capabilities of various adsorbents. The adsorption isotherm is the relationship between the amount of adsorbate adsorbed on the adsorbent and the equilibrium concentrations of adsorbate at constant temperatures.

According to the Langmuir model, the adsorbent surface has numerous active interaction sites for the adsorption process. It is concerned with the relationship between adsorbed material and its equilibrium concentration. The linear form of Langmuir adsorption isotherm equation (3) model is described, allowing for the processes of adsorption and desorption of molecules on the surface.

$$\frac{C_e}{q_e} = \frac{1}{bq_{\max}} + \frac{C_e}{q_{\max}}, \quad (3)$$

where q_e denotes the mass of adsorbate adsorbed over adsorbent (mg/g); C_e denotes the equilibrium concentration of adsorbate acquired in the liquid phase after adsorption (mg/L); q_{\max} denotes the maximum adsorbate that can be adsorbed (monolayer capacity) (mg/g); and b denotes the Langmuir

isotherm constant (L/mg). In another manner, using the equation given next, the separation factor (dimensionless), also known as the RL factor or the equilibrium parameter, was calculated from the empirical constant b .

$$R_L = \frac{1}{1 + bC_O} \quad (4)$$

The value of R_L in equation (4) indicates the adsorbent's suitability for adsorption.

It is a relationship between the amount of an adsorbate absorbed per unit weight of adsorbent and the adsorbate equilibrium concentration (C_e) in the fluid. The Freundlich model, unlike the Langmuir model, is based on multilayer adsorption and may be expressed as

$$\frac{X}{M} = KC_e^{1/n}, \quad (5)$$

where K and n are the Freundlich coefficients, X is the weight of adsorbate adsorbed on M unit weight of adsorbent, and C_e is the adsorbate equilibrium concentration. However, it is possible to express the equilibrium condition as

$$\log(q_e) = \log(k_f) + \frac{1}{n \log(C_e)}, \quad (6)$$

where q_e is the mass of adsorbate adsorbed over adsorbent (mg/g); K_f is the Freundlich capacity factor (units determined by q_e); C_e is the equilibrium concentration of adsorbate in the liquid phase after adsorption (mg/L); and n is Freundlich intensity parameter. The intercept and slope of a plot of $\log(q_e)$ versus $\log(C_e)$ can be used to determine the value of coefficients k_f and n .

3. Results and Discussion

3.1. Characterization of WT. Proximate and TGA analyses were conducted on waste tires to determine the physical and thermal decomposition property of the precursor. Table 1 shows the ash content and moisture content characteristics of the waste tire.

During the burning of the tire, the fugitive matter in tires is composed of polymeric polymers produced from natural rubber and styrene-butadiene, whereas the fixed ash is composed of black carbon used in tire manufacturing. Many nonblack pitches are additionally utilized in tire production. Ashes also come from these nonblack fillers.

The ash content of the precursor, as presented in Figure 1(a), was 6.1% when the temperature was 400°C, whereas the ash content of the sample decreased to 5.8% when the temperature was 500°C. However, the difference between the two temperatures is the time, the 500°C treated sample reached the required ash content more quickly than that of 400°C.

To explain this phenomenon, the ash component materials should be considered. For instance, one of the nonblack fillers, calcium carbonate, will decompose as the temperature increases in calcium oxide and carbon dioxide, which brings about significant changes in the ash content of the tire. Likewise, many black and nonblack fillers will be

TABLE 1: Comparison of moisture and ash contents of this work with other studies.

Ash content (% m/m)	Moisture content (% m/m)	References
6.1	0.46	This work
2.4–20.12	0.4–2.1	[35]
9.99 ± 0.52	0.89 ± 0.01	[36]

converted to volatile components like carbon dioxide, sulfur dioxide, and other light hydrocarbon components which decrease the ash content portion of the sample more quickly. Carbon blacks are supposed to be less reactive due to their tight circumferential structure. However, an increment in temperature leads to a change in the rigidity structure of the carbon black. In general, ash content indicates the amount of inorganic matter existing in a particular matter.

Figure 1(b) illustrates the thermogravimetric profile of the waste tire sample used in the experiment. The analysis represents 1.9% of weight loss in the temperature range of 50–275°C due to moisture release and loss of some volatile matter. After the temperature of 275°C, there was a sudden fall in the weight up to 28.1% of the sample tire was lost, up to the temperature of around 400°C. The premises of these losses were found to be natural and synthetic rubbers. These rubbers started to decompose and escape. After the temperature of 400°C, the further falling of the temperature continued up to 500°C. The carbon black, which is one of the components of a waste tire, is responsible due to its decomposition. The last 3.6% weight loss exists after 500°C; with these, finally some carbon black residue and ash will remain. In addition, significant carbon black residual was observed in most environments except air and oxygen-enhanced atmospheres, as a 3.6% residual existence is expected.

3.2. Preparation of WTAC and Methylene Blue Removal

3.2.1. Effect of Temperature. From Figure 2(a), as the temperature climbs from 500 to 900°C, the yield of WTAC decreases, suggesting that the conversion of rubber matter to elemental porous carbon continues and decreases. The yield had reduced from 52.61% at 500°C to 30.11% at 900°C. It could also be explained that increasing temperature affected the yield which indicates that the carbon materials were being lost with volatile components. A similar result was presented by Shah et al. [37].

From the methylene blue removal temperature bar, it could be understood that increasing temperature from 500 to 700°C leads to an increment of MB removal from 70.21% to 89.42%. At a temperature higher than 700°C, somehow maximum and nearly uniform MB removal was found. The minimum removal of MB has been calculated at 800°C (88.56%). The reduction has been linked to the harsh thermal treatment, which results in the breaking of cross-links in the carbon matrix, as well as a reorganization of carbonaceous aggregates and pore collapse. These lead to some inefficiency in the adsorption of MB at a temperature of and beyond 800°C. A similar result was presented by the author using different types of precursors [38]. Teng et al.

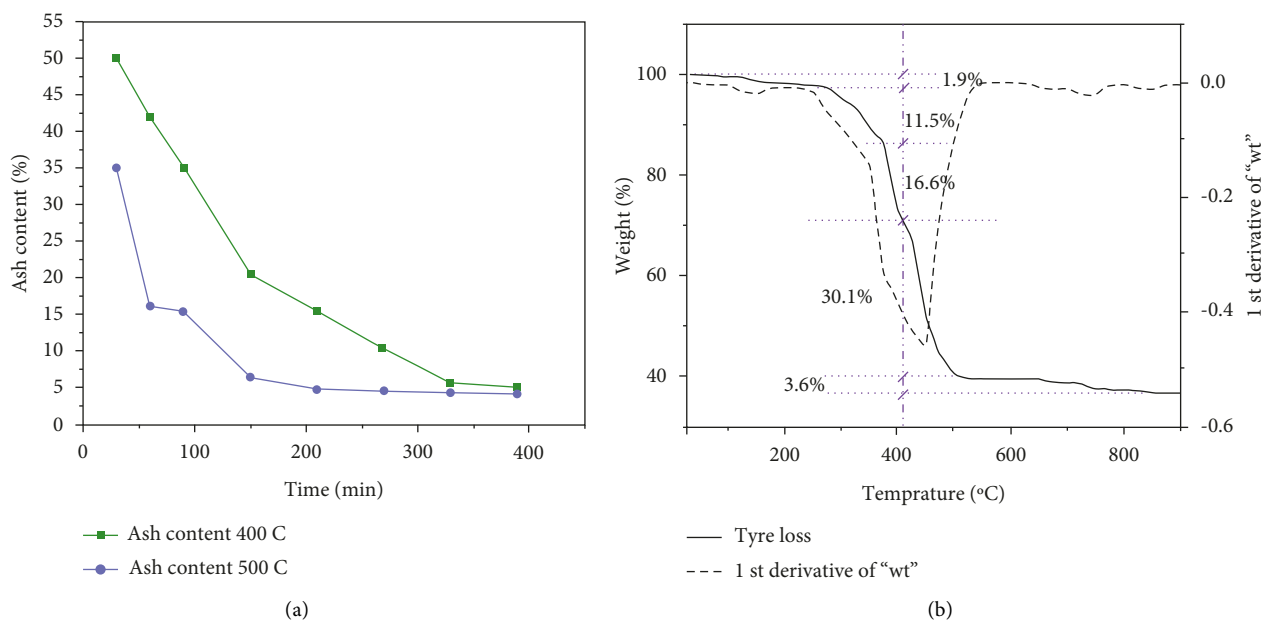


FIGURE 1: Ash content versus time graph of (a) waste tire precursor and (b) TGA analysis and its derivative curves.

had focused on increased surface area and pore volume at a temperature range of 700–800°C [26].

3.2.2. Effect of Impregnation Ratio. The effect of the impregnation ratio on AC yield was studied by varying its amount from 0 to 4 and making another value constant (Figure 2(b)). When the impregnation ratio increases from 0 to 2, the result indicated that yield increases from 35.28% to 44.66%, then suddenly shoots down to 36.86% when the impregnation ratio was 4. This is due to the continuous degradation of tire components due to the increment of corrosive ethanolic KOH amount. This degradation is the result of the formation of CO₂ and CO. As a result, a carbon component of the tire will be lost due to these chemical transformations. This finding is in line with Al-Rahbi and Williams [39].

The case of MB removal showed that the maximum adsorption attained is at an impregnation ratio value of 0, around 89.41%. After that, the MB removal percentage begins to decrease directly. The reason behind this is that according to Teng et al. [26], the increment of IR further from it leads to a decrement of the micropore volume of the WTAC due to the removal of carbon atoms from the pore walls and decrement of surface area.

3.2.3. Effect of Impregnation Time. The impregnation time had a crucial effect on the yield and adsorption of MB. The longer the impregnated tire and the chemicals stayed together within a heating media, the capability of the WTAC to remove MB has been increasingly large valued up to an impregnation time of 24 h (88.91%). At the impregnation time of 12 h, the MB removal was 88.37% and 85.71% at 6 h of impregnation time. However, further increment of the impregnation time will not affect the process positively. The

minimum amount of MB removal was found at 48 h of time, that is, 84.47% (Figure 2(c)).

Further increment in impregnation time after 24 h will result in loss of material (sample tire and ethanolic KOH) and energy, but with an enhancement of WTAC yield. The yield of WTAC gradually increases from 38.74% to 41.45%, when the impregnation time runs from 6 to 12 h. Beyond 24 h, a maximum yield percentage of 42.65% was found at 48 h. Results on the effect of impregnation time on the yield and MB removal have not been yet reported by authors on tire-based activated carbon. Unlike many precursors that decreased their yield with increasing impregnation time, this tire-based material had enhanced the yield with an increment in impregnation time. The possible reasons might be the existence of potassium and potassium oxides being formed as a side reaction with a long time of impregnation. The impregnation time selected for optimization was 12–36 h, due to its maximum removal of MB and gaining the advantage of energy and raw material cost.

3.2.4. Effect of KOH Concentration. Initially, the MB removal was 89.76% at the concentration of 1 M of the concentration of KOH. Then, the MB removal increased up to a concentration of 3 M (89.89%), and beyond that it has boomed up to 90.13% at 4 M and again had decreased to 89.56% at 5 M (Figure 2(d)). The reason behind these figures is that increasing the concentration of KOH has a direct effect on porosity, especially on the broadening of the created and existing pores where the MB is expected to be attached, as explained by Teng et al. [26].

The effect of the concentration of KOH, especially using ethanol as a solvent, was not studied before on tires. KOH concentration had roles in the development of pores. The enhancement in KOH would fasten the rate of reaction in addition to the quantity of the pores increment. Although

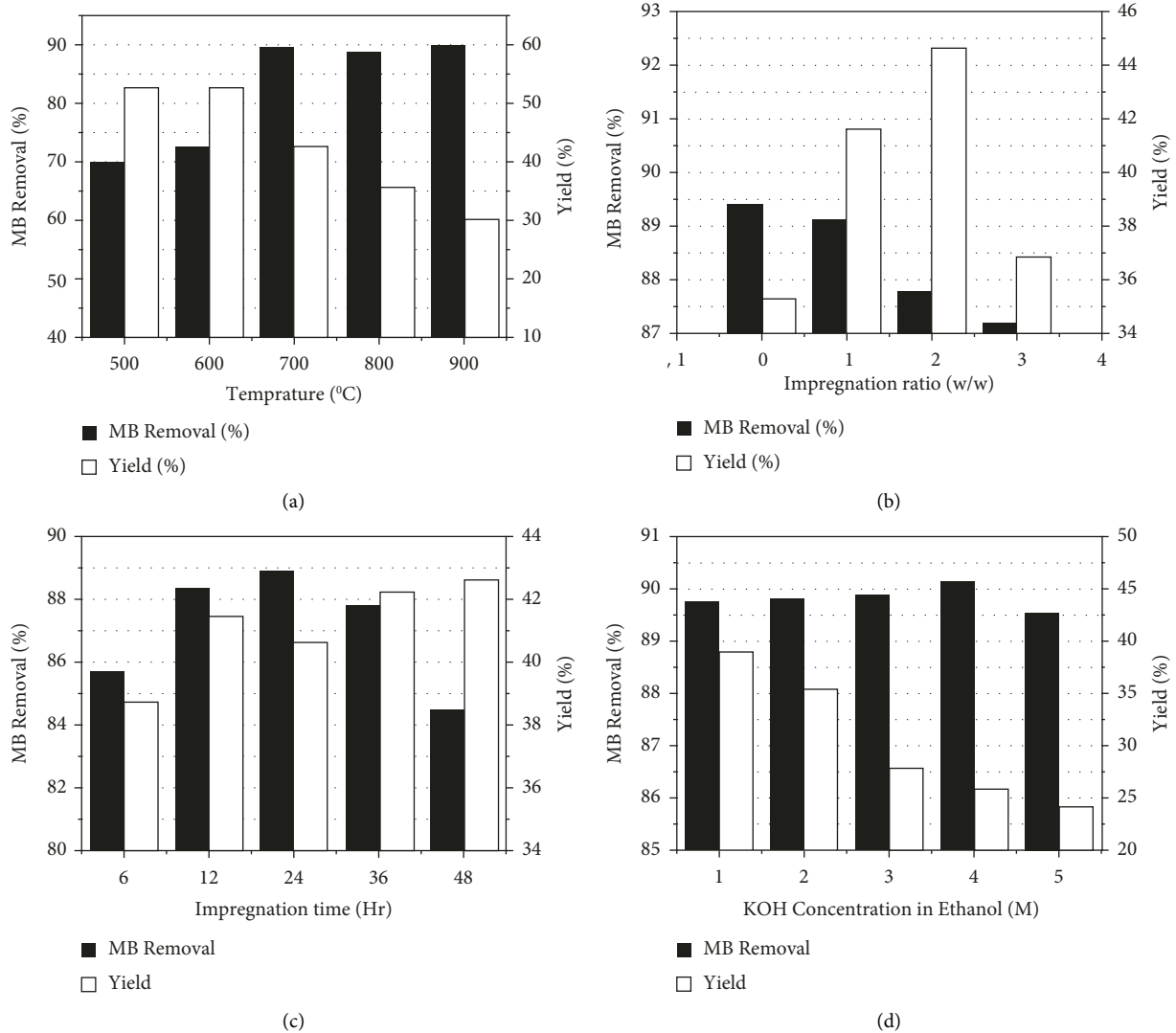


FIGURE 2: Effect of temperature at constant KOH concentration of 2 M in 97% ethanol, impregnation ratio of 1, impregnation time of 24 h, and holding time of 2 h (a); the effect of impregnation ratio at constant KOH concentration of 2 M in 97% ethanol, carbonization temperature of 800°C, impregnation time of 24 h, and holding time of 2 h (b); the effect of impregnation time at constant KOH concentration of 2 M in 97% ethanol, carbonization temperature of 800°C, impregnation ratio of 1, and holding time of 2 h (c); effect of KOH concentration in 97% ethanol at constant carbonization temperature of 800°C, impregnation ratio of 1, impregnation time of 24 h, and holding time of 2 h (d) on MB removal and yield.

there was an extreme range of KOH concentration beyond which the MB adsorbing capacity WTAC is reduced. Since the excessive concentration of KOH might result in side reactions between KOH and carbon which change the pore structure of already developed pores as expressed by Chowdhury [40].

As Figure 2(d) shows, KOH concentration has increased from 1 to 5 M, and the carbon yield of the WTAC decreases strictly (from 39.09% to 24.23%). The strict decrement in the yield has been because of the increment in KOH concentration that is directly related to an increment in the amount of potassium within the solution, which is highly ready to react with the existing carbonaceous compounds within the tire to form carbon-containing gases that were entering the atmosphere and as a result, increases the loss of carbon

material in different forms. Furthermore, increasing the concentration of KOH also increases the corrosivity of the ethanolic KOH, which is highly capable of positively influencing the MB removal ability, but negatively influencing the yield of the waste tire-based carbonaceous materials as understood from Figure 2(d).

3.3. Demineralization Experiments (Surface Area Enhancement). The demineralization experiments were made so that the surface area of WTAC could be increased from 53 m²/g. In this experimentation, inorganic minerals such as ZnO were removed from the pores and polymeric resins of rubber, which could lead to enhancement of the surface area. The main aim of these experiments was to

reduce the ash content inside WTAC so that the amount of inorganic matter was reduced in the WTAC. In this demineralization process, H_2SO_4 had the next minimum ash extract (7.39%) among the demineralized sample and had a surface area of $115.9 \text{ m}^2/\text{g}$. On the other hand, NaOH had a maximum surface area of $227.2 \text{ m}^2/\text{g}$ and an ash extract value of 10.65%, which is the highest value of ash content that is not preferable (Figure 3). Compromising the trade-off between the two solvents, NaOH and H_2SO_4 (1 : 1) ratio was used to demineralize waste tire-based activated carbon, and the result as clearly indicated on the bar (Figure 3) had minimum ash content (6.512%) and maximum surface area ($257.8 \text{ m}^2/\text{g}$) that was highly preferable for further adsorption process.

Comparably similar results of ash content were presented by Henry [41] and had elaborated the improved amount of $\text{NaOH-H}_2\text{SO}_4$ demineralization as the existence of two oxides that are added to a tire while fabrication, specifically zinc oxide (ZnO) and silicon dioxide. Considering SiO_2 , electronegativity among the atoms is very durable, triggering a solid covalent bond instead of ionic bonds. SiO_2 does not dissociate due to a lack of ionic connections and hence cannot react with dissociated acid of the H^+ ion. SiO_2 is somewhat acidic compound that must be reacted with a strong alkali, such as NaOH . The energy provided by the NaOH utilized in the subsequent extractions is sufficient to break the silicon-oxygen link, resulting in sodium silicon deoxidate ($\text{Na}_2\text{O.nSiO}_2$).

3.4. Characterization of WTAC

3.4.1. SEM Imaging of WTAC and Demineralized Waste Tire-Based Activated Carbon. As it could be understood from Figure 4, a well-developed porous structure could be observed in these demineralized samples than those of nondemineralized samples. Comparably the HNO_3 demineralized samples were found to be less porous than the mixed H_2SO_4 and NaOH demineralized samples. Increasing the degree of magnification further showed the surface structure more. Roughs, gullies, and frequent hills had been observed on the SEM images of both demineralized samples. However, the effect of the solvent had been seen in the images. This roughness and frequent hilliness were found to a more extent on NaOH and H_2SO_4 demineralized samples. These indicated the effectiveness of the demineralizing solvent to bring chemical changes inside the openings of the waste tire-based activated carbon so that unwanted chemicals could be removed.

For the HNO_3 demineralized sample (Figures 4(a) and 4(b)), the distribution of opening area and distribution of opening diameter were $23.5699 \mu\text{m}^2$ and $5.3574 \mu\text{m}$ on average, respectively. However, minimum and maximum opening areas of $5.187 \mu\text{m}^2$ and $77.377 \mu\text{m}^2$ were calculated, respectively, whereas a minimum opening diameter of $1.761 \mu\text{m}$ and a maximum opening diameter of $22.642 \mu\text{m}$ were recorded from the SEM imaging.

In addition, for $\text{H}_2\text{SO}_4+\text{NaOH}$ demineralized sample (Figures 4(b) and 4(d)), the distribution of opening area and distribution of opening diameter were $1.978 \mu\text{m}^2$ and

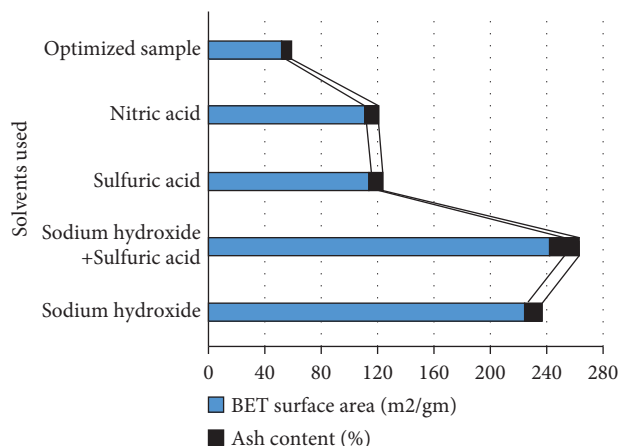


FIGURE 3: The amount of ash extracted in wt.% from WTAC solvents/lixiviant.

$2.015 \mu\text{m}$ on average, respectively. However, minimum and maximum opening areas of $0.06 \mu\text{m}^2$ and $11.761 \mu\text{m}^2$ were calculated, respectively, whereas a minimum opening diameter of $0.635 \mu\text{m}$ and a maximum opening diameter of $4.949 \mu\text{m}$ were recorded from the SEM imaging. From these findings, it could be concluded that the HNO_3 demineralized sample possesses a larger opening area and diameter than that of the acid-base demineralized sample.

Comparatively, with the WTAC sample which is not demineralized (Figure 4(e)), SEM images of WTAC samples indicated significant differences in the sample's morphology than the demineralized samples in both solvents. It was observed that the treatment improved the porous structure of the treated products. It was evident that sodium hydroxide treatment is able of reducing the inorganic components of carbon, concerning the major inorganic species, zinc.

3.4.2. XRD of Demineralized Sample. The XRD pattern of the demineralized WTAC (DEWTAC) is eluted in Figure 5(a). The XRD pattern showed a broad peak A at 2θ of around 25° , indicating the existence of amorphous carbon. While the peaks B, C, and D showed the presence of SiC mineral. These peaks were found at $2\theta = 44.02^\circ$, 64.5° , and 77.66° corresponding to side spacing of 2.0554 \AA , 1.4435 \AA , and 1.2285 \AA , respectively. The crystalline sizes of B, C, and D were 12.901 nm , 13.915 nm , and 3.0688 nm in the same order. The crystallinity of the HNO_3 DMWTAC has been calculated by the percentage of the area of crystalline peaks (390.78) to the area of all peaks (7018.88). The crystallinity of the sample was 5.567%.

3.4.3. Spectrum Study of the DMWTAC. Figure 5(b) shows the wavelength versus absorbance spectrum of untreated MB and treated MB with different samples that are demineralized by various solvents. The above blue curve indicated the untreated MB solution having 10 mg/L of concentration. The maximum absorbance value has been found by it since it had got maximum concentration. Upon stepping one step down the MB removal capability of the phosphoric acid

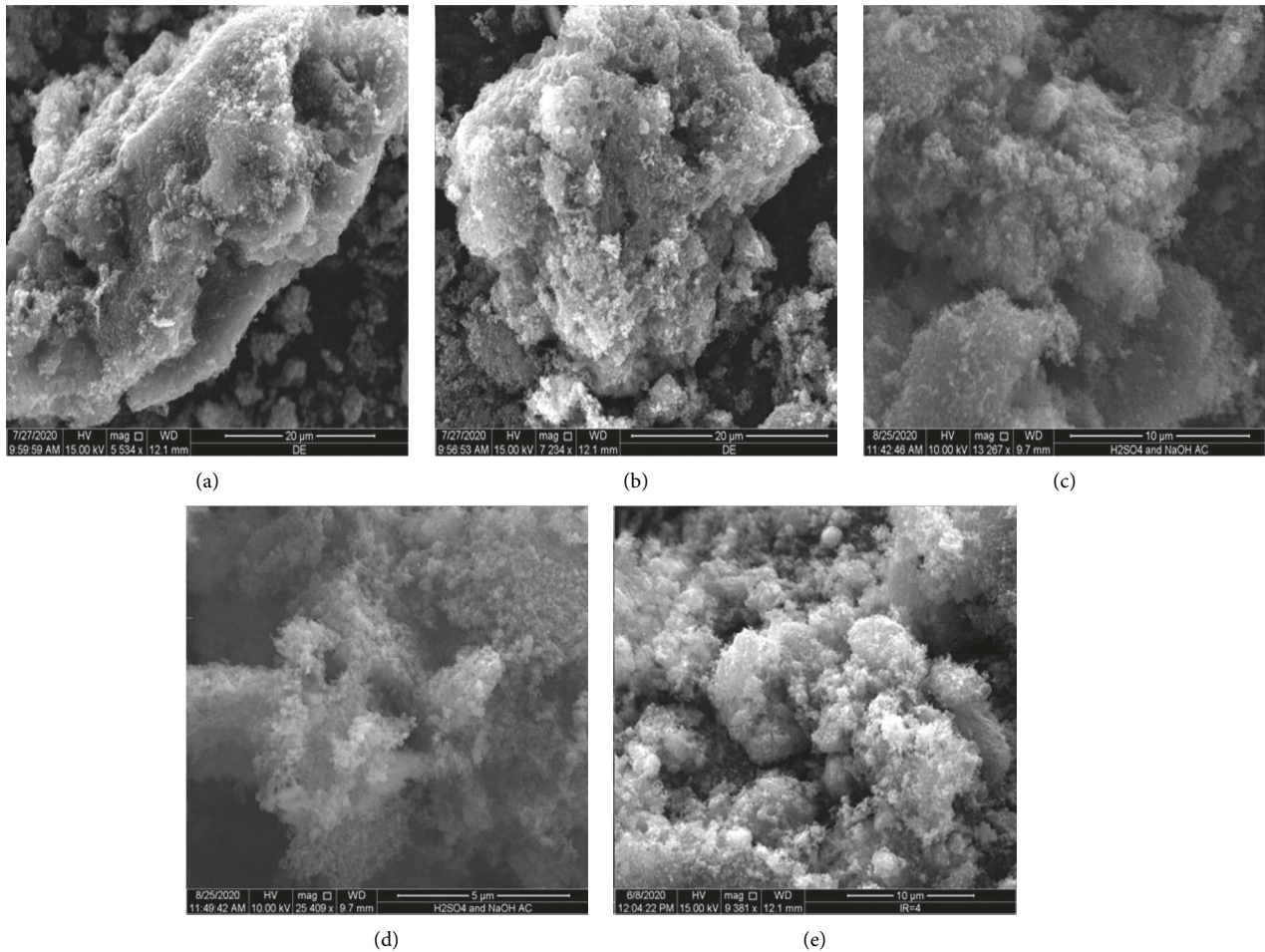


FIGURE 4: A SEM image for a sample demineralized with solvent (only HNO_3) with different magnifications of $7234\times$ (a) and $5534\times$ (b) and demineralized with solvent (H_2SO_4 and NaOH in 1:1 ratio) with different magnifications of $13,287\times$ (c) and $25,400\times$ (d) and not the demineralized sample of WTAC (e).

demineralized sample has been plotted, and next to the untreated sample it has the highest absorbance, which means that more concentrated MB was found from it. The purest of all treated MB solutions were found from the treatment of NaOH and H_2SO_4 demineralized samples, the green line, since it had a minimum concentration of MB, the absorbance was found to be small. The absorbance of MB was minimum by the use of sodium hydroxide and sulfuric acid in demineralized samples, the reason behind this was, first, the unwanted minerals found within the tire were removed from the demineralized samples, which helps to enhance the porosity of the samples, and second, the surface area of the prepared carbonaceous compound has increased from about 50 to $250\text{ m}^2/\text{g}$. This helps to give maximum affinity to the activated carbon to the removal of the MB dye.

Even if similar experiments have not been done, to compare the result, according to Dargo et al., decolorization experiments are dependent on ion exchange and adsorption process [24]. The adsorption process is dependent solely on the surface characteristics or property of the adsorbent and its internal surface area and porosity of it. That was why, the absorbance decreased as demineralized samples were used,

which is, in turn, the indication of the decrement in the final concentration of the treated sample as well as the increment in the percentage reduction of the MB in the remediated solution.

3.4.4. Atomic Absorption Spectroscopical Studies. The non-demineralized sample has been found to have a greater number of metals than the waste tire crumb. According to Khodaie et al., because chemical solvents have a difficult time accessing and dissolving metals trapped in the organic matrix of tire rubber, the tire may be resistant to chemical treatments [42]. However, with a WTAC sample (not demineralized), the organic matrix was already burnt off while pyrolysis, which leaves the ash of inorganic compounds exposed on the char surface. The concentration of some elements for instance aluminum, calcium, and magnesium might increase in the WTAC sample than that of the waste tire in raw (Table 2).

Comparing the WTAC and DMWTAC in terms of reduction of metallic concentration, Zn metal is the one that has decreased significantly having a percentage reduction in

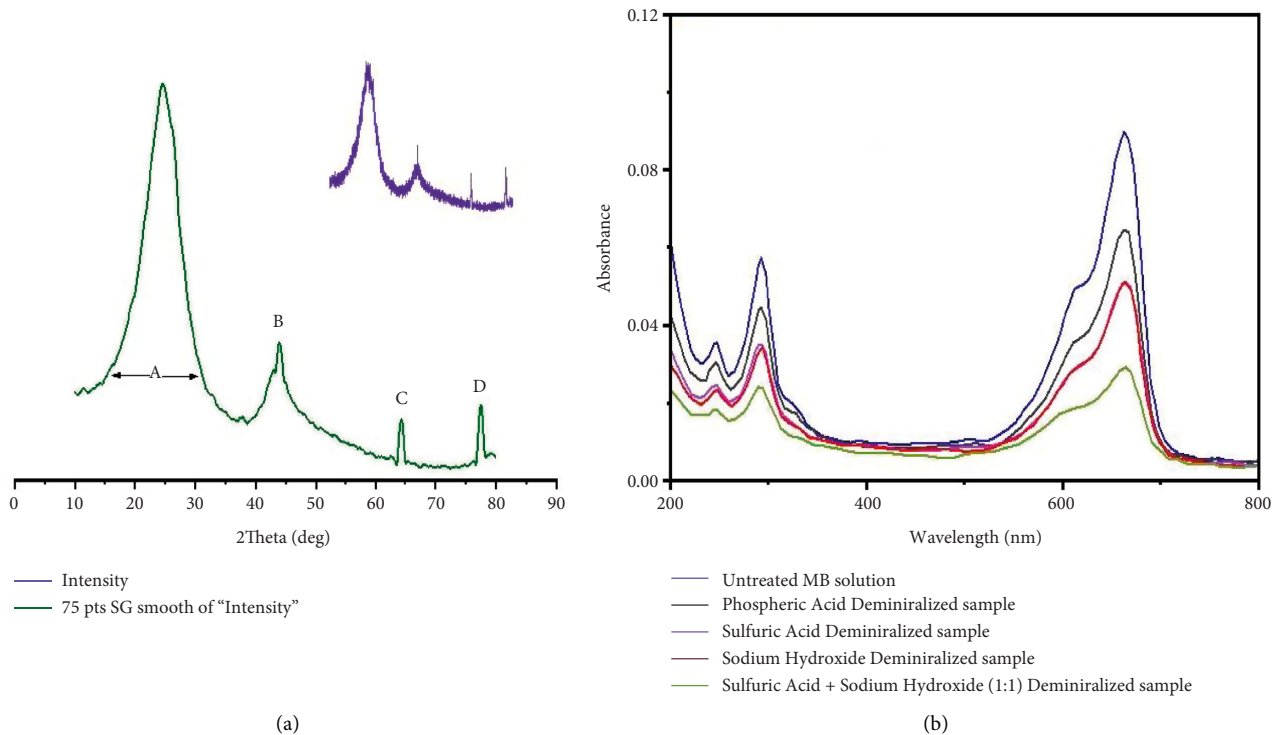


FIGURE 5: XRD pattern of the demineralized sample by HNO_3 (a) and wavelength versus absorbance spectrum of untreated methylene blue and treated methylene blue with different samples that are demineralized by various solvents (b).

TABLE 2: AAS results of four metals Ca, Mg, Zn, and Al.

Metals	Conc. of WTAC (mg/L)	Conc. of ($\text{NaOH} + \text{H}_2\text{SO}_4$) DMWTAC (mg/L)	Percent of metal reduced
Ca^{2+}	81.75	58.90	27.95
Mg^{2+}	3.785	3.526	6.843
Zn^{2+}	10.76	6.048	43.79
Al^{3+}	2.351	1.588	32.45

the concentration of 43.79%. Up next was Al, which had attained a 32.45% reduction, followed by Ca and Mg, which were reduced to 27.95% and 6.843%, respectively (Table 2). As stated in Section 2.5, this reduction is mainly due to the dissociation chemistry of solvent (NaOH plus H_2SO_4) on the optimized activated carbon sample.

3.5. MB Adsorption by DMWTAC

3.5.1. Variation of Initial MB Concentration. There are enough adsorption sites accessible for MB adsorption at lower MB concentrations. As MB concentration gets higher, relatively fewer available sites will be there which leads to a reduction in adsorption of MB on the surface of DMWTAC. Investigations were done at constant adsorption conditions (0.2 g, $\text{PH} = 2$, $\text{rpm} = 400$, and 30 min) by changing the initial MB concentration from 10 to 80 mg/L (Figure 6(a)). The maximum reduction efficiency of MB found at 10 mg/L of concentration is about 94.55%, and directly the % reduction decreased up to 70 mg/L, which is 90.13%, beyond this value there was no significant decrement or increment in % reduction of MB.

Simply, with the decrement in pollutant concentration in the aqueous solution, adsorbate molecules had more capability to react with the existing active sites on DMWTAC, and the adsorption rate was enhanced. The same scenarios could be seen with different authors [43, 44].

On the contrary, the amount adsorbed in mg/g increases directly and linearly with an increment in initial MB concentration. Initially, the amount adsorbed was 7.1 mg/g at 10 mg/L, which later boomed to 53.5 mg/g at 80 mg/L, signifying that the quantity of total MB buildup grew as starting concentrations rose. Rahman et al. had found the same result and explained this situation, due to more contact of adsorbent sites with MB [45].

Based on the facts presented in Figure 6(a), it could be concluded that one method of enhancing the MB removal is the dilution of the existing solution in response to the change in initial MB concentration. The majority of MB in the solution may come into touch with DMWTAC active sites at low concentrations. However, because the active sites are already filled, when the concentration is raised, all MB particles will be unable to make contact with them.

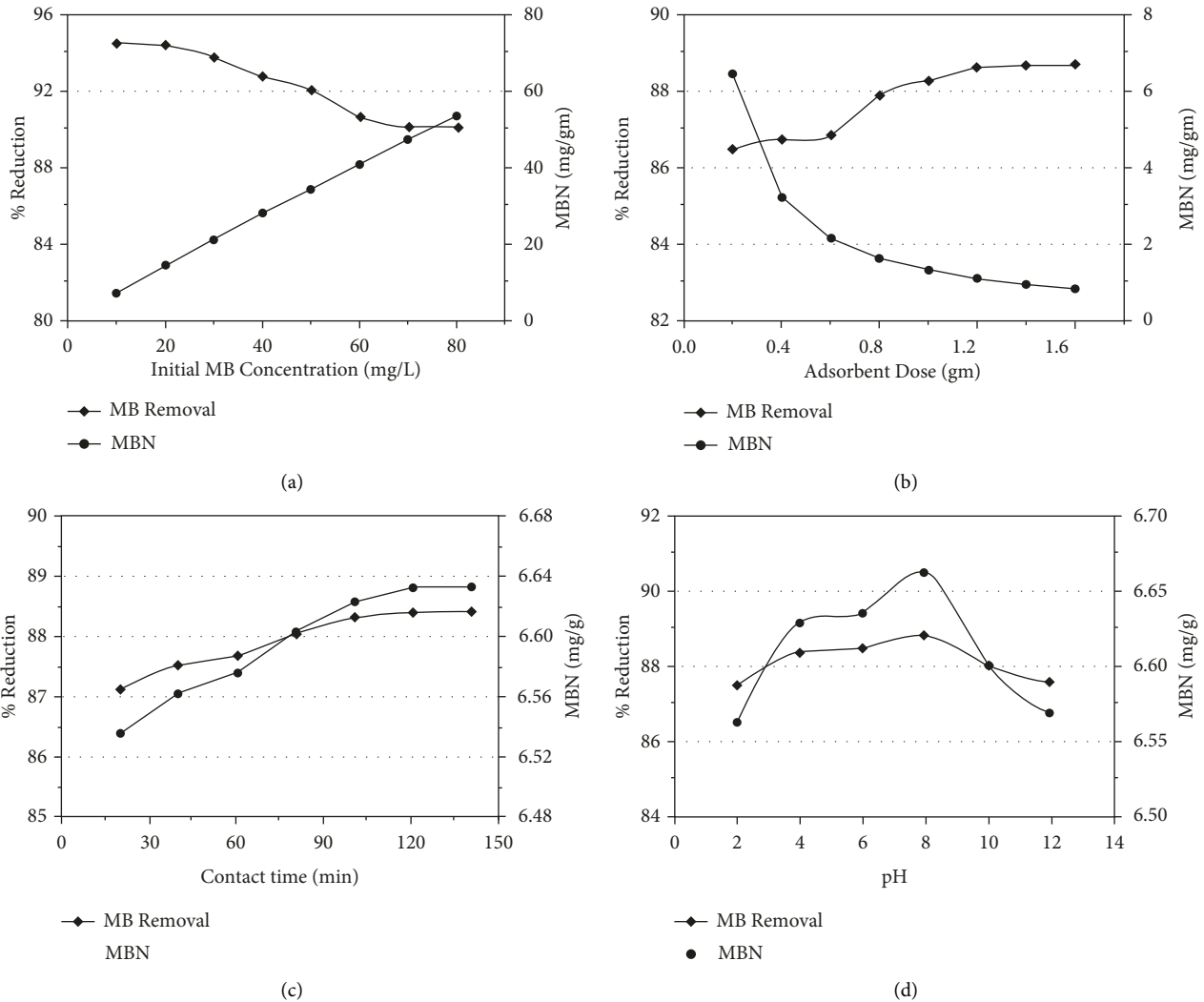


FIGURE 6: The effect of initial MB concentration at constant pH of 2, adsorbent dose of 0.2 g, contact time of 30 min, the temperature of 20°C, and 400 rpm stirrer rotation (a); the effect of DMWTAC amount at constant pH of 2, initial concentration of 10 mg/L, the contact time of 30 min, the temperature of 20°C, and 400 rpm stirrer rotation (b); the effect of contact time at constant pH of 2, adsorbent dose of 0.2 g, initial concentration of 10 mg/L, the temperature of 20°C, and 400 rpm stirrer rotation (c); the effect of variation of pH at a constant initial concentration of 10 mg/L, adsorbent dose of 0.2 g, the contact time of 30 min, the temperature of 20°C, and 400 rpm stirrer rotation (d) on the % reduction of MB and MBN.

3.5.2. Variation of DMWTAC Amount. From Figure 6(b), it could be observed that percentage reduction had increased with an increasing amount in the adsorbent dosage from 0.2 g of WTAC dosage (86.52%) to 1.6 g of DMWTAC dosage (88.75%). However, 1.4 g will be the equilibrium dosage, with a percent reduction of 88.71%. After reaching this point, the percentage removal remained constant, without showing a significant change in the increase of % reduction. In this phenomenon, increasing adsorbent dosage did not lead to higher MB number (MBN) because of the overload of activated carbon area is decreased, in other words, the MB adsorbate is got lost. The same was detected that with an upsurge in quantity from 0.01 to 0.1 g/100 ml, the removal efficiency varied from 35% to 90% for flower waste biomass [46].

Quantity (mg/g) of MB adsorbed reduces with the growth in dosage similar to Ghosh et al. [47]. When the DMWTAC

quantity was 0.2 g, the quantity adsorbed was 6.5 mg/g, and at equilibrium point (0.95 mg/g) the quantity adsorbed diminished to 0.83 mg/g. Khodaie et al. [42] statement may be attributed to two reasons: first, the increase in sorbent dose at constant MB concentration and volume will lead to unsaturation of adsorption sites via the adsorption process, and second, due to particulate interaction such as aggregation resulting from a high adsorbent dose. Aggregation may lead to a decrease in the total surface area of the adsorbent. This was in correspondence with the removal of MB using *Jatropha curcas* when the adsorbent dosage was varied from 0.01 g/100 ml to 0.05/100 ml [44].

3.5.3. Variation of Contacting Time. In adsorption processes, contact time is influenced by involving the movement of dye from the bulk of the solution to the surface

DMWTAC and diffusion of dye over the layer of the boundary to the surface and into the interior pores of the adsorbent [48]. Experiments were done at constant adsorption conditions (0.2 g, pH = 2, rpm = 400, and initial concentration = 10 mg/L) by changing the contact time from 20 to 140 min (Figure 6(c)).

As seen in Figure 6(c), a rapid % reduction in the DMWTAC has been observed at the initial stages of the adsorption and the percentage of adsorption has increased from 87.14% to 88.41% within 120 min. Such uptakes indicated the capacity of the adsorbent toward dye molecules is through chemisorption (electrostatic attraction and hydrogen bonding) [49]. Following these uptakes, the adsorbent's capacity was depleted, and adsorption was swapped by dye molecule movement from the adsorbent particles' exterior to inner regions. The same results were also obtained from Corda and Kini [50]. Initially, the percentage of removal is higher due to the availability of the adsorbent sites, and then it is reduced as a result of the saturation of the sites and the pore diffusion becomes slow [47].

In the same manner, the MBN increases rapidly by contacting time and becomes stable. When the time has increased from 20 min to 140 min, the MBN was enhanced from 6.5 to 6.63 mg/g. Quick diffusion toward the external surface of the WTAC was rapidly followed by quick pore diffusion toward the intraparticle matrix for the attainment of rapid equilibrium. This is why equilibrium had attained at 120 min, beyond which there was a significant change in both % reduction and MBN.

3.5.4. Variation of Solution pH. As the pH of the MB solution climbed, the positive charge at the solution interface decreased and the adsorbent surface became negatively charged. As a result, the cationic dye adsorption increased [51]. As a result, the OH⁻ content in the solution was high for this investigation at high pH values, and the adsorbent surface was negatively charged. Consequently, MB dye, which is positively charged, could be attracted to the adsorbent surface. At lower pH, the adsorbed quantity of MB dye has reduced for the reason that the external area of the adsorbent was more protonated and competitive adsorption happened among H⁺ protons and positively charged MB dye at the surface sites [42]. From Figure 6(d), it could be understood that the percentage reduction of MB had increased with pH value increment. It could be manifested by the fact that the percentage reduction of MB had enhanced from 87.5% to 88.83% as pH varies from 2 to 8 (where the maximum amount of adsorptive reduction of MB was calculated). This is due to the reason discussed above. As it can be seen from Figure 6(d), a pH value of 8 can be considered optimum pH, since percentage removal showed a decreasing trend beyond pH of 8. After the pH of 8, removal percentage of MB had decreased up to 87.6%, where the pH was exactly 12. This is due to the repulsive force between the adsorbent and adsorbate as illustrated by Saheed et al. [44]. Similar trends in the effect of initial solution pH were reported by Barai and Jha [52] and Kanawade et al. [53].

Similarly, the MBN has increased from 6.56 mg/g to 6.66 mg/g from a pH value of 2 to 8, whereas these values had decreased to 6.57 mg/g when the pH, later on, becomes 12. Due to the reasons discussed above, the amount of MB accumulated on the surface of the adsorbent could not increase beyond these amounts as also seen by Ghosh et al. [47].

3.5.5. Variation of Temperature. To analyze the effect of the change in temperature on the % reduction of MB dye over DMWTAC, numerous experiments have been performed at temperatures of 20°C, 30°C, 40°C, 50°C, and 60°C. Figure 7 presents the impact of temperature on the adsorption of MB dye onto WTAC at constant adsorption conditions (0.2 g, pH = 2, rpm = 400, contacting time = 30 min, and initial concentration = 10 mg/L (Figure 7)). The % reduction of MB had decreased with an increase in temperature. This recommends that the adsorption of MB on WTAC follows an exothermic process. Similar results have been reported by Dargo et al. [24]. According to Figure 7, the higher % reduction of MB had been found at 20°C (88.3%) and diminished to 60°C (87.67%), while MBN was decreased from 6.62 to 6.57 mg/L, with an increment in temperature from 20 to 60°C. Increasing the temperature is known to increase the rate of diffusion of the adsorbate molecules across the external boundary layer and in the internal pores of the adsorbent particle [42]. However, in this case, an increment in temperature diminishes the rate of diffusion of adsorbate molecules.

3.6. Adsorption Mechanism

3.6.1. Adsorption Isotherm. To understand the adsorption mechanism, investigating the adsorption isotherm of MB dye is very important. Adsorption isotherm defines the distribution of adsorbed molecules on the adsorbent interface [42]. This model assumes uniform energies of adsorption onto the surface and no transmigration of adsorbate in the plane of the surface [54]. The linear regression method was applied to determine the constants of the Langmuir and Freundlich models. Temkin isotherm model indicated a relatively good correlation ($R^2 = 0.97$) as shown in Table 3. This showed that the adsorption process occurs at a specific homogeneous adsorption site on an adsorbent surface. Specifically for Langmuir isotherm, for different Co values (10–50 mg/L), R_L values were in between 0 and 1 ($0 < R_L < 1$) (Table 3). This indicates that the process is favorable.

3.6.2. Adsorption Kinetics. Pseudo-first order and pseudo-second order are the models used to examine the kinetics of the metal adsorption process [55]. As presented in Table 4, the values of correlation coefficient R^2 and the pseudo-second-order adsorption mechanism have been found to be the preferred kinetic model, and the overall rate of the MB adsorption process appeared to be controlled by the chemical reaction.

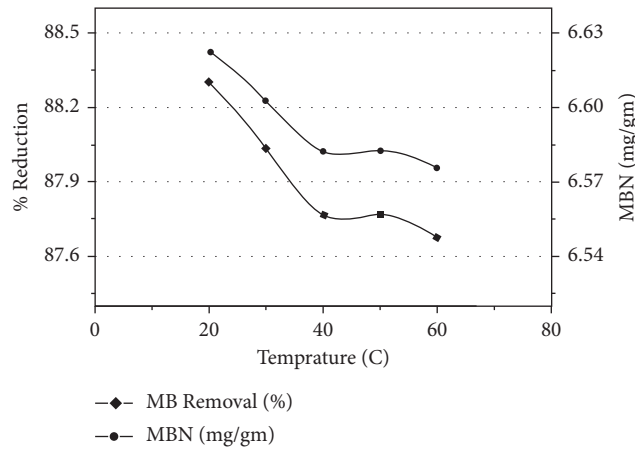


FIGURE 7: The effect of temperature on the % reduction of MB and MBN at constant pH of 2, adsorbent dose of 0.2 g, contact time of 30 min, initial concentration of 10 mg/L, and 400 rpm stirrer rotation.

TABLE 3: Parameters obtained by Langmuir, Freundlich, and Temkin isotherms for methylene blue dye adsorption by WTAC.

Isotherm	R^2	Q_m	K_L	Equations
Langmuir	0.96	73.53	0.13	$Y = 0.014X + 0.11$
Freundlich	0.96	1.68	10.28	$Y = 0.59X + 1.01$
Temkin	0.97	16.43	1.27	$Y = 16.43X + 3.87$

TABLE 4: Adsorption kinetic parameters for removal of MB by WTAC.

Kinetics	R^2	Q_e	K_1
First-order kinetics	0.98	0.017	-0.052
Second-order kinetics	0.99	11.16	-0.027

TABLE 5: Comparison of adsorption capacity of DMWTAC with other adsorbents reported in different studies.

Adsorbent	Removal Capacity (Q_{max} (mg/g))	Reference
DMWTAC	53	This study
Modified polysaccharide	48	[56]
Rice husk	40	[57]
Hydrolyzed oak sawdust	67.78	[58]
Peanut husk	42.13	[59]

3.7. Regeneration and Adsorption Capacity of the Adsorbent.

The regeneration was made using the solid-phase extraction, and eight cycles of MB concentration were analyzed. The retained MB was flushed with 1 M HNO_3 . However, the activated carbon sample was capable to be reprocessed eight times, and the regeneration was comparably consistent with a slight decrement in the removal efficiency of MB.

Table 5 provides the adsorption capacity of this study and other previously studied data. Accordingly, the obtained removal capacity of this study was found to be significant as the other studied data listed in Table 5.

4. Conclusions

This study has explored the preparation and characterization of WTAC by chemical activation using ethanolic KOH and its capability for MB removal. The experimental outcomes indicated that waste tires can be used to prepare AC and its BET surface area could be enhanced by intensive chemical activation/demineralization of the prepared WTAC. The removal of MB could be influenced by impregnation ratio, impregnation time, KOH concentration, and carbonization temperature. The BET surface area was improved from $53 \text{ m}^2/\text{g}$ to $257 \text{ m}^2/\text{g}$ through an intensive demineralization process. The XRD and AAS analysis indicated that a high amount of metals/minerals were removed from the optimized samples. SEM image of the activated carbon showed an irregular slit structure micrograph which supports the formation of well-developed pores on the AC surface. The adsorption capacity of the WTAC was checked by MB adsorption through the batch adsorption technique at different adsorption conditions. The various adsorption parameters such as the effect of pH, initial MB concentration, adsorbent/WTAC dosage, temperature, and contact time on the % reduction of MB and MBN, where the optimum conditions for adsorption of MB onto WTAC were found to be 1.2 g adsorbent dosage, 120 min contact time, pH of 8, the temperature of 20°C , and initial dye concentration of 10 mg/L. Adsorption investigation indicated that DMWTAC can be successfully utilized for the removal of a pollutant called MB due to the existence of binding active sites.

Data Availability

The data used to support the findings of this study are included in the article.

Conflicts of Interest

The authors declare that they have no conflicts of interest.

Acknowledgments

The authors would like to thank the Department of Chemical Engineering, College of Biological and Chemical Engineering, Addis Ababa Science and Technology University, Addis Ababa, Ethiopia.

References

- [1] Y. Asrat, A. T. Adugna, M. Kamaraj, and S. M. Beyan, "Adsorption phenomenon of *Arundinaria alpina* stem-based activated carbon for the removal of lead from aqueous solution," *Journal of Chemistry*, vol. 2021, Article ID 5554353, 9 pages, 2021.
- [2] S. M. Beyan, S. V. Prabhu, T. T. Sissay, and A. A. Getahun, "Sugarcane bagasse based activated carbon preparation and its adsorption efficacy on removal of BOD and COD from textile effluents: RSM based modeling, optimization and kinetic aspects," *Bioresource Technology Reports*, vol. 14, Article ID 100664, 2021.
- [3] Y. Luka, "The promising precursors for development of activated carbon: agricultural waste materials- A review," *International Journal of Advanced Science and Research*, vol. 4, pp. 45–59, 2018.
- [4] M. Moyo, L. Chikazaza, B. C. Nyamunda, and U. Guyo, "Adsorption batch studies on the removal of Pb (II) using maize tassel based activated carbon," *Journal of Chemistry*, vol. 2013, Article ID 508934, 8 pages, 2013.
- [5] V. K. Gupta and Suhas, "Application of low-cost adsorbents for dye removal—a review," *Journal of Environmental Management*, vol. 90, no. 8, pp. 2313–2342, 2009.
- [6] F. A. López, T. A. Centeno, O. Rodríguez, and F. J. Alguacil, "Preparation and characterization of activated carbon from the char produced in the thermolysis of granulated scrap tyres," *Journal of the Air & Waste Management Association*, vol. 63, no. 5, pp. 534–544, 2013.
- [7] B. Acevedo and C. Barriocanal, "Texture and surface chemistry of activated carbons obtained from tyre wastes," *Fuel Processing Technology*, vol. 134, pp. 275–283, 2015.
- [8] T. A. Saleh and G. I. Danmaliki, "Adsorptive desulfurization of dibenzothiophene from fuels by rubber tyres-derived carbons: kinetics and isotherms evaluation," *Process Safety and Environmental Protection*, vol. 102, pp. 9–19, 2016.
- [9] S. M. Wabaidur, M. A. Khan, M. R. Siddiqui et al., "Oxygenated functionalities enriched MWCNTs decorated with silica coated spinel ferrite—a nanocomposite for potentially rapid and efficient de-colorization of aquatic environment," *Journal of Molecular Liquids*, vol. 317, Article ID 113916, 2020.
- [10] Z. A. Alothman, A. H. Bahkali, M. A. Khiyami et al., "Low cost biosorbents from fungi for heavy metals removal from wastewater," *Separation Science and Technology*, vol. 55, no. 10, pp. 1766–1775, 2020.
- [11] M. A. Khan, A. A. Alqadami, S. M. Wabaidur et al., "Oil industry waste based non-magnetic and magnetic hydrochar to sequester potentially toxic post-transition metal ions from water," *Journal of Hazardous Materials*, vol. 400, Article ID 123247, 2020.
- [12] S. Tadesse and D. Ambo, "Removal of basic dye from aqueous medium using activated carbon from *Erythrina brucei*, *Arundinaria alpina* and *Manihot esculenta*," *Food Science and Quality Management*, vol. 86, pp. 19–27, 2019.
- [13] X. Duan, C. Srinivasakannan, X. Wang, F. Wang, and X. Liu, "Synthesis of activated carbon fibers from cotton by microwave induced H₃PO₄ activation," *Journal of the Taiwan Institute of Chemical Engineers*, vol. 70, pp. 374–381, 2017.
- [14] K. Zuo, K. Wang, R. M. DuChanois et al., "Selective membranes in water and wastewater treatment: role of advanced materials," *Materials Today*, vol. 50, pp. 516–532, 2021.
- [15] D. Deemter, I. Oller, A. M. Amat, and S. Malato, "Advances in membrane separation of urban wastewater effluents for (pre) concentration of microcontaminants and nutrient recovery: a mini review," *Chemical Engineering Journal Advances*, vol. 11, Article ID 100298, 2022.
- [16] K. A. Landry, P. Sun, C. H. Huang, and T. H. Boyer, "Ion-exchange selectivity of diclofenac, ibuprofen, ketoprofen, and naproxen in ureolyzed human urine," *Water Research*, vol. 68, pp. 510–521, 2015.
- [17] Z. Ye, X. Yin, L. Chen et al., "An integrated process for removal and recovery of Cr (VI) from electroplating wastewater by ion exchange and reduction–precipitation based on a silica-supported pyridine resin," *Journal of Cleaner Production*, vol. 236, Article ID 117631, 2019.
- [18] I. Ali, O. M. L. Alharbi, Z. A. AlOthman, A. M. Al-Mohaimed, and A. Alwarthan, "Modeling of fenuron pesticide adsorption on CNTs for mechanistic insight and removal in water," *Environmental Research*, vol. 170, pp. 389–397, 2019.
- [19] E. R. Kenawy, A. A. Ghfar, S. M. Wabaidur et al., "Cetyltrimethylammonium bromide intercalated and branched polyhydroxystyrene functionalized montmorillonite clay to sequester cationic dyes," *Journal of Environmental Management*, vol. 219, pp. 285–293, 2018.
- [20] A. A. Alqadami, M. A. Khan, M. R. Siddiqui, and Z. A. Alothman, "Development of citric anhydride anchored mesoporous MOF through post synthesis modification to sequester potentially toxic lead (II) from water," *Microporous and Mesoporous Materials*, vol. 261, pp. 198–206, 2018.
- [21] T. A. Amibo, S. M. Beyan, and T. M. Damite, "Production and optimization of bio-based silica nanoparticle from teff straw (*Eragrostis tef*) using RSM-based modeling, characterization aspects, and adsorption efficacy of methyl orange dye," *Journal of Chemistry*, vol. 2022, Article ID 9770520, 15 pages, 2022.
- [22] S. M. Beyan, T. A. Ambio, V. P. Sundramurthy, C. Gomadurai, and A. A. Getahun, "Adsorption phenomenon for removal of Pb (II) via teff straw based activated carbon prepared by microwave-assisted pyrolysis: process modelling, statistical optimisation, isotherm, kinetics, and thermodynamic studies," *International Journal of Environmental Analytical Chemistry*, vol. 102, pp. 1–22, 2022.
- [23] T. A. Amibo, S. M. Beyan, and T. M. Damite, "Novel lanthanum doped magnetic teff straw biochar nanocomposite and optimization its efficacy of defluoridation of groundwater using rsm: a case study of hawassa city, Ethiopia," *Advances in Materials Science and Engineering*, vol. 2021, Article ID 9444577, 15 pages, 2021.
- [24] H. Dargo, N. Gabbiye, and A. Ayalew, "Removal of methylene blue from waste water using activated carbon prepared from rice husk," *International Journal of Innovation Science and Research*, vol. 9, pp. 317–325, 2015.
- [25] S. Bhattacharya, N. Bar, B. Rajbansi, and S. K. Das, "Adsorptive elimination of Cu (II) from aqueous solution by chitosan-nanoSiO₂ nanocomposite—adsorption study, MLR, and GA modeling," *Water, Air, & Soil Pollution*, vol. 232, no. 4, p. 161, 2021.
- [26] H. Teng, Y.-C. Lin, and L.-Y. Hsu, "Production of activated carbons from pyrolysis of waste tires impregnated with

- potassium hydroxide," *Journal of the Air & Waste Management Association*, vol. 50, no. 11, pp. 1940–1946, 2000.
- [27] D. Zahn, P. Mucha, V. Zilles et al., "Identification of potentially mobile and persistent transformation products of REACH-registered chemicals and their occurrence in surface waters," *Water Research*, vol. 150, pp. 86–96, 2019.
- [28] S. M. Beyan, S. V. Prabhu, T. A. Ambio, and C. Gomadurai, "A statistical modeling and optimization for Cr (VI) adsorption from aqueous media via teff straw-based activated carbon: isotherm, kinetics, and thermodynamic studies," *Adsorption Science and Technology*, vol. 2021, Article ID 7998069, 16 pages, 2021.
- [29] S. M. Beyan, S. V. Prabhu, T. A. Ambio, and C. Gomadurai, "A statistical modeling and optimization for Cr (VI) adsorption from aqueous media via teff straw-based activated carbon: isotherm, kinetics, and thermodynamic studies," *Adsorption Science and Technology*, vol. 2022, Article ID 7998069, 16 pages, 2022.
- [30] T. A. Amibo, S. M. Beyan, M. Mustefa, V. P. Sundramurthy, and A. B. Bayu, "Development of nanocomposite based antimicrobial cotton fabrics impregnated by Nano SiO₂ loaded AgNPs derived from *Eragrostis teff* straw," *Materials Research Innovations*, vol. 76, pp. 1–10, 2021.
- [31] T. K. Mumecha, B. Surafel Mustefa, S. Venkatesa Prabhu, and F. T. Zewde, "Alkaline protease production using eggshells and membrane-based substrates: process modeling, optimization, and evaluation of detergent potency," *Engineering and Applied Science Research*, vol. 48, pp. 171–180, 2021.
- [32] S. M. Beyan, T. A. Amibo, and V. P. Sundramurthy, "Development of anchote (*Coccinia abyssinica*) starch-based edible film: response surface modeling and interactive analysis of composition for water vapor permeability," *Journal of Food Measurement and Characterization*, vol. 16, no. 3, pp. 2259–2272, 2022.
- [33] S. M. Beyan, T. A. Amibo, S. V. Prabhu, and A. G. Ayalew, "Production of nanocellulose crystal derived from enset fiber using acid hydrolysis Coupled with ultrasonication, isolation, statistical modeling, optimization, and characterizations," *Journal of Nanomaterials*, vol. 2021, Article ID 7492532, 12 pages, 2021.
- [34] W. Kidus Tekleab, S. M. Beyan, S. Balakrishnan, and H. Admassu, "Chicken feathers based Keratin extraction process data analysis using response surface-box-Behnken design method and characterization of keratin product," *Current Applied Science and Technology*, vol. 20, pp. 163–177, 2020.
- [35] S. M. R. Costa, D. Fowler, G. A. Carreira, I. Portugal, and C. M. Silva, "Production and upgrading of recovered carbon black from the pyrolysis of end-of-life tires," *Materials*, vol. 15, no. 6, p. 2030, 2022.
- [36] R. B. González-González, L. T. González, S. Iglesias-González et al., "Characterization of chemically activated pyrolytic carbon black derived from waste tires as a candidate for nanomaterial precursor," *Nanomaterials*, vol. 10, no. 11, pp. 2213–2222, 2020.
- [37] J. Shah, M. R. Jan, F. Maboob, and M. Shahid, "Conversion of waste tyres into carbon black and their utilization as adsorbent," *Journal of the Chinese Chemical Society*, vol. 53, no. 5, pp. 1085–1089, 2006.
- [38] S. Valliammai, Y. Subbareddy, K. S. Nagaraja, and B. Jeyaraj, "Removal of Methylene blue from aqueous solution by activated carbon of *Vigna mungo* L and *Paspalum scrobiculatum*: equilibrium, kinetics and thermodynamic studies," *Indian Journal of Chemical Technology*, vol. 24, pp. 134–144, 2017.
- [39] A. S. Al-Rahbi and P. T. Williams, "Production of activated carbons from waste tyres for low temperature NO_x control," *Waste Management*, vol. 49, pp. 188–195, 2016.
- [40] Z. Z. Chowdhury, *Preparation, Characterization and Adsorption Studies of Heavy Metals onto Activated Adsorbent Materials Derived from Agricultural Residues*, Universiti Malaya, Kuala Lumpur, Malaysia, 2013.
- [41] K. L. Henry, *Upgrading Pyrolytic Tyre Char through Acid-Alkali Demineralisation*, Stellenbosch University, Stellenbosch, South Africa, 2015.
- [42] M. Khodaie, N. Ghasemi, B. Moradi, and M. Rahimi, "Removal of methylene blue from wastewater by adsorption onto ZnCl₂ Activated corn husk carbon equilibrium studies," *Journal of Chemistry*, vol. 2013, Article ID 383985, 6 pages, 2013.
- [43] M. A. Baghapour, "Removal of methylene blue from aqueous solutions by waste paper derived activated carbon," *J Heal. Sci Surveill. Sys.* vol. 1, pp. 48–56, 2013.
- [44] I. O. Saheed, F. A. Adekola, and G. A. Olatunji, "Sorptions study of methylene blue on activated carbon prepared from *Jatropha curcas* and *Terminalia catappa* seed coats," *Journal of the Turkish Chemical Society, Section A: Chemistry*, vol. 4, no. 1, p. 375, 2016.
- [45] M. A. Rahman, S. M. R. Amin, and A. M. S. Alam, "Removal of methylene blue from waste water using activated carbon prepared from rice husk," *Dhaka University Journal of Science*, vol. 60, no. 2, pp. 185–189, 2012.
- [46] N. Ertugay and E. Malkoc, "Adsorption isotherm, kinetic, and thermodynamic studies for methylene blue from aqueous solution by needles of *Pinus sylvestris* L, Polish," *Journal of Environmental Studies*, vol. 23, pp. 1995–2006, 2014.
- [47] K. Ghosh, N. Bar, A. B. Biswas, and S. K. Das, "Removal of methylene blue (aq) using untreated and acid-treated eucalyptus leaves and GA-ANN modelling," *Canadian Journal of Chemical Engineering*, vol. 97, no. 11, pp. 2883–2898, 2019.
- [48] A. Q. Alorabi, "Effective removal of malachite green from aqueous solutions using magnetic nanocomposite: synthesis, characterization, and equilibrium study," *Adsorption Science and Technology*, vol. 2021, Article ID 2359110, 15 pages, 2021.
- [49] S. A. Mousavi, M. Mehralian, M. Khashij, and S. Parvaneh, "Methylene blue removal from aqueous solutions by activated carbon prepared from *N. Microphyllum* (AC-NM): RSM analysis, isotherms and kinetic studies," *Global NEST Journal*, vol. 19, pp. 697–705, 2017.
- [50] N. C. Corda and M. S. Kini, "A review on adsorption of cationic dyes using activated carbon," *MATEC Web of Conferences*, vol. 144, Article ID 02022, 2018.
- [51] M. Naushad, G. Sharma, and Z. A. Alothman, "Photodegradation of toxic dye using Gum Arabic-crosslinked-poly (acrylamide)/Ni (OH)₂/FeOOH nanocomposites hydrogel," *Journal of Cleaner Production*, vol. 241, Article ID 118263, 2019.
- [52] D. R. Barai and V. K. Jha, "Preparation of activated charcoal adsorbent from waste tire," *Scientific World*, vol. 10, pp. 80–83, 2012.
- [53] S. M. Kanawade, R. W. Gaikwad, A. M. Blue, and C. W. Hyacinth, "Removal of methylene blue from effluent by using activated carbon and water hyacinth as adsorbent," *International Journal of Chemical Engineering and Applications*, vol. 2, pp. 317–319, 2011.
- [54] T. Ahmed, W. Noor, O. Faruk, M. C. Bhoumick, and M. T. Uddin, "Removal of methylene blue (MB) from waste

water by adsorption on jackfruit leaf powder (JLP) in continuously stirred tank reactor,” *Journal of Physics: Conference Series*, vol. 1086, Article ID 012012, 2018.

- [55] I. Ghosh, S. Kar, T. Chatterjee, N. Bar, and S. K. Das, “Removal of methylene blue from aqueous solution using *Lathyrus sativus* husk: adsorption study, MPR and ANN modelling,” *Process Safety and Environmental Protection*, vol. 149, pp. 345–361, 2021.
- [56] A. T. Paulino, M. R. Guilherme, A. V. Reis, G. M. Campese, E. C. Muniz, and J. Nozaki, “Removal of methylene blue dye from an aqueous media using superabsorbent hydrogel supported on modified polysaccharide,” *Journal of Colloid and Interface Science*, vol. 301, no. 1, pp. 55–62, 2006.
- [57] V. Vadivelan and K. V. Kumar, “Equilibrium, kinetics, mechanism, and process design for the sorption of methylene blue onto rice husk,” *Journal of Colloid and Interface Science*, vol. 286, no. 1, pp. 90–100, 2005.
- [58] M. M. Abd El- Latif and A. M. Ibrahim, “Adsorption, kinetic and equilibrium studies on removal of basic dye from aqueous solutions using hydrolyzed Oak sawdust,” *Desalination and Water Treatment*, vol. 6, no. 1-3, pp. 252–268, 2009.
- [59] J. Song, W. Zou, Y. Bian, F. Su, and R. Han, “Adsorption characteristics of methylene blue by peanut husk in batch and column modes,” *Desalination*, vol. 265, no. 1-3, pp. 119–125, 2011.